Title

Specific tumor labeling enhanced by polyethylene glycol linkage of near infrared dyes conjugated to a chimeric anti-carcinoembryonic antigen antibody in a nude mouse model of human pancreatic cancer

Journal

Journal of Biomedical Optics, 19(10)

ISSN

1083-3668

Authors

Maawy, Ali A
Hiroshima, Yukihiko
Zhang, Yong
et al.

Publication Date

2014-06-02

DOI

10.1117/1.jbo.19.10.101504

Peer reviewed

Journal of Biomedical Optics

SPIEDigitalLibrary.org/jbo

Specific tumor labeling enhanced by polyethylene glycol linkage of near infrared dyes conjugated to a chimeric anti-carcinoembryonic antigen antibody in a nude mouse model of human pancreatic cancer

Ali A. Maawy
Yukihiko Hiroshima
Yong Zhang
George A. Luiken
Robert M. Hoffman
Michael Bouvet

SPIE

Specific tumor labeling enhanced by polyethylene glycol linkage of near infrared dyes conjugated to a chimeric anti-carcinoembryonic antigen antibody in a nude mouse model of human pancreatic cancer

Ali A. Maawy,[a] Yukihiko Hiroshima,[a,b,c] Yong Zhang,[b] George A. Luiken,[d] Robert M. Hoffman,[a,b] and Michael Bouvet[a,e,*]
[a]University of California San Diego, Department of Surgery, 200 West Arbor Drive, No. 8220, San Diego, California 92103-8220
[b]AntiCancer, Inc., 7917 Ostrow Street, San Diego, California 92111
[c]Yokohama City University, Yokohama City 236-0004, Japan
[d]OncoFluor, Inc., 1211 Alameda Boulevard, Coronado, California 92118
[e]VA San Diego Healthcare System, 3350 La Jolla Village Drive, San Diego, California 92161

Abstract. Labeling of metastatic tumors can aid in their staging and resection of cancer. Near infrared (NIR) dyes have been used in the clinic for tumor labeling. However, there can be a nonspecific uptake of dye by the liver, lungs, and lymph nodes, which hinders detection of metastasis. In order to overcome these problems, we have used two NIR dyes (DyLight 650 and 750) conjugated to a chimeric anti-carcinoembryonic antigen antibody to evaluate how polyethylene glycol linkage (PEGylation) can improve specific tumor labeling in a nude mouse model of human pancreatic cancer. The conjugated PEGylated and non-PEGylated DyLight 650 and 750 dyes were injected intravenously into non-tumor-bearing nude mice. Serum samples were collected at various time points in order to determine serum concentrations and elimination kinetics. Conjugated PEGylated dyes had significantly higher serum dye concentrations than non-PEGylated dyes ($p = 0.005$ for the 650 dyes and $p < 0.001$ for the 750 dyes). Human pancreatic tumors subcutaneously implanted into nude mice were labeled with antibody-dye conjugates and serially imaged. Labeling with conjugated PEGylated dyes resulted in significantly brighter tumors compared to the non-PEGylated dyes ($p < 0.001$ for the 650 dyes; $p = 0.01$ for 750 dyes). PEGylation of the NIR dyes also decreased their accumulation in lymph nodes, liver, and lung. These results demonstrate enhanced selective tumor labeling by PEGylation of dyes conjugated to a tumor-specific antibody, suggesting their future clinical use in fluorescence-guided surgery. [DOI: 10.1117/1.JBO.19.10.101504]

Keywords: chimeric anti-carcinoembryonic antigen; antibody; near infrared dyes; nude mice; pancreatic cancer; imaging; polyethylene glycol linkage; polyethylene glycol linkage.

Paper 140174SSR received Mar. 16, 2014; revised manuscript received May 3, 2014; accepted for publication May 5, 2014; published online Jun. 2, 2014.

1 Introduction

We have previously used chimeric anti-carcinoembryonic antigen (CEA) antibodies conjugated with visible or near-infrared fluorescent dyes for imaging pancreatic cancer in orthotopic nude mouse models.[1] The longer wavelength dyes in the 650 and 750 nm wavelength range had increased depth of penetration and ability to detect the smallest tumor deposits and provided the highest tumor to background ratios, resistance to hemoglobin quenching, and specificity compared with shorter wavelength dyes in the 488 and 550 nm range. However, there was nonspecific uptake in the liver and lymph nodes of the near infrared (NIR) dyes, which could limit their use in specific tumor imaging. Since polyethylene glycol (PEG) conjugation can alter the pharmacokinetics and biodistribution of molecules,[2–7] we hypothesized that the polyethylene glycol linkage (PEGylation) of NIR dyes conjugated with anti-CEA antibodies could enable enhanced tumor labeling in a nude mouse model of human pancreatic cancer, which is the subject of the present report.

*Address all correspondence to: Michael Bouvet, E-mail: mbouvet@ucsd.edu

2 Materials and Methods

2.1 *Cell Culture*

The human pancreatic cancer cell line BxPC-3 was obtained from the American Type Culture Collection (ATCC) (Manassas, Virginia). Cells were maintained in RPMI 1640 medium supplemented with 10% fetal bovine serum and 2-mM glutamine. (Gibco-BRL, Life Technologies, Inc., Grand Island, New York.) All cells were cultured at 37°C in a 5% CO_2 incubator.

2.2 *Antibody-Dye Conjugation*

Chimeric anti-CEA antibody (Aragen Biosciences, Morgan Hill, California) was conjugated to PEGylated and non-PEGylated DyLight dyes (Thermo Fisher Scientific, Rockford, Illinois) per manufacturer specifications, ensuring a minimum dye:protein ratio of at least 4:1 (Fig. 1). Protein:dye

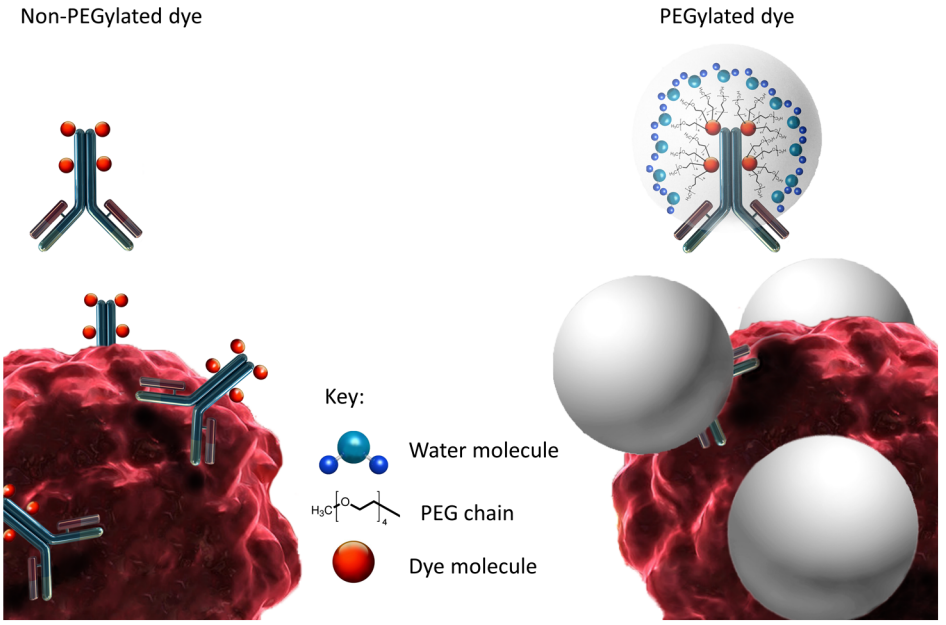

Fig. 1 Schematic depiction of the difference in structure of the PEGylated and non-PEGylated dye-mAb complexes.

concentrations and ratios were confirmed using a NanoDrop Spectrophotometer (Thermo Fisher Scientific, Rockford, Illinois).

2.3 *Animals*

Athymic nu/nu nude mice (AntiCancer, Inc., San Diego, California) between 4 and 6 weeks of age were maintained in a barrier facility on high efficiency particulate air (HEPA)-filtered racks. The animals were fed with autoclaved laboratory rodent diet (Teckland LM-485; Western Research Products, Orange, California). All surgical procedures and imaging were performed with the animals anesthetized by intramuscular injection 0.02 ml of 50% ketamine, 38% xylazine, and 12% acepromazine maleate. When inhalational anesthesia was required, 99% isoflurane and 100% oxygen were delivered via a vaporizer. All animal studies were conducted under an Anti-Cancer Institutional Animal Care and Use Committee (IACUC) approved protocol and in accordance with the principles and procedures outlined in the National Institutes of Health Guide for the Care and Use of Animals under Assurance Number A3873-1. Animals received buprenorphine (0.10 mg/kg ip) immediately prior to surgery and once a day over the next 3 days to ameliorate pain.

2.4 *Tumor Implantation*

After confluence, BxPC-3 human pancreatic cancer cells (1×10^6) were injected subcutaneously into the flanks of nude mice and allowed to engraft and grow over a period of 4 to 6 weeks. Tumors were then harvested and tumor fragments (1 mm^3) were implanted subcutaneously into each quadrant of the dorsal surface in nude mice. The tumor fragments were allowed to engraft and grow over a period of about 4 weeks until they were 10 to 20 mm^3 in volume.

2.5 *Serum Concentration Determination*

A 100-nmol/μL solution of free dye was prepared from DyLight 650 and 750 in phosphate buffered saline (PBS). The solution was serially diluted 10-fold and 200-μL samples of each concentration were placed in a well on a 96-well plate. The 96-well plate was then placed in a plate reader (Tecan Sunrise Remote Microplate Reader, Männedorf, Switzerland), and the absorbance determined for DyLight 650 and 750 at 672 and 776 nm, respectively. A plot of absorbance versus concentration served as a standard curve to determine future serum concentrations based on absorbance.

DyLight 650 or 750 (2.5 nmol) conjugated to the anti-CEA antibody was injected into the tail vein of 60 nude mice. Three mice were then subsequently sacrificed at various time points by exsanguination from cardiac puncture at 5 min, 30 min, 1 h, 3 h, 6 h, and 24 h after conjugated dye injection. Blood samples were allowed to sit in room air in 1.5-ml Eppendorf tubes for 15 min to allow for coagulation. Blood samples were subsequently centrifuged at 5000 rpm for 5 min in a Beckman microfuge 18 (Beckman Coulter Inc., Brea, California) and the serum supernatant collected. Each serum sample (200 μL) was placed in a 96-well plate in a plate reader to evaluate serum absorbance at 672 and 776 nm for the DyLight 650 and 750 samples, respectively. Dye concentrations were determined from their standard curves and plotted over time.

2.6 *Tissue Biodistribution*

Dye (2.5 nmol) conjugated to anti-CEA antibody was injected into the tail vein of 20 nude mice divided into four groups of five. The mice were sacrificed after 24 h by CO_2 inhalation and cervical dislocation. Liver and lung tissue (5 mg) were obtained from each mouse. In each case, PBS (200 μL) was added to the tissue, which was subsequently homogenized by sonication with a Branson 450 sonifer (Branson Ultrasonics Corp., Danbury, Connecticut) at 20 KHz, until complete liquefaction.

The homogenized tissue was subsequently centrifuged at 5000 rpm for 3 min in a Beckman microfuge 18 (Beckman Coulter Inc., Brea, California) and the supernatant with dye collected. Each sample (100 μL) was placed in a 96-well plate and diluted to 200 μL. The sample was placed in the plate reader and the absorbance from each sample was measured. Using standard curves, the sample concentration of dye was determined.

2.7 *Animal Imaging*

Mice were imaged using the Olympus OV100 (Olympus Corp., Tokyo, Japan), containing an MT-20 light source (Olympus Biosystems, Planegg, Germany), and DP70 CCD camera (Olympus Corp., Tokyo, Japan). The OV100 was used due to its unique ability to accomplish high fidelity fluorescence imaging with variable magnification capabilities that allow for imaging of not only the whole animal, but also at the subcellular level. The instrument incorporates a unique combination of a high numerical aperture and long working distance. Four individually optimized objective lenses, parcentered, and parfocal provide a 10^5 fold magnification range for seamless imaging of the entire body down to the subcellular level without disturbing the animal.[8] In addition, openings on the machine allow for delivery of inhalational anesthesia to the animal without allowing entry of outside light. This allows for capturing high quality *in vivo* images with minimal morbidity to the animal by avoiding anesthetic injections. All images were analyzed using Image-J (National Institute of Health, Bethesda, Maryland) and were processed with the use of Photoshop Elements 11 (Adobe Systems Inc., San Jose, California).

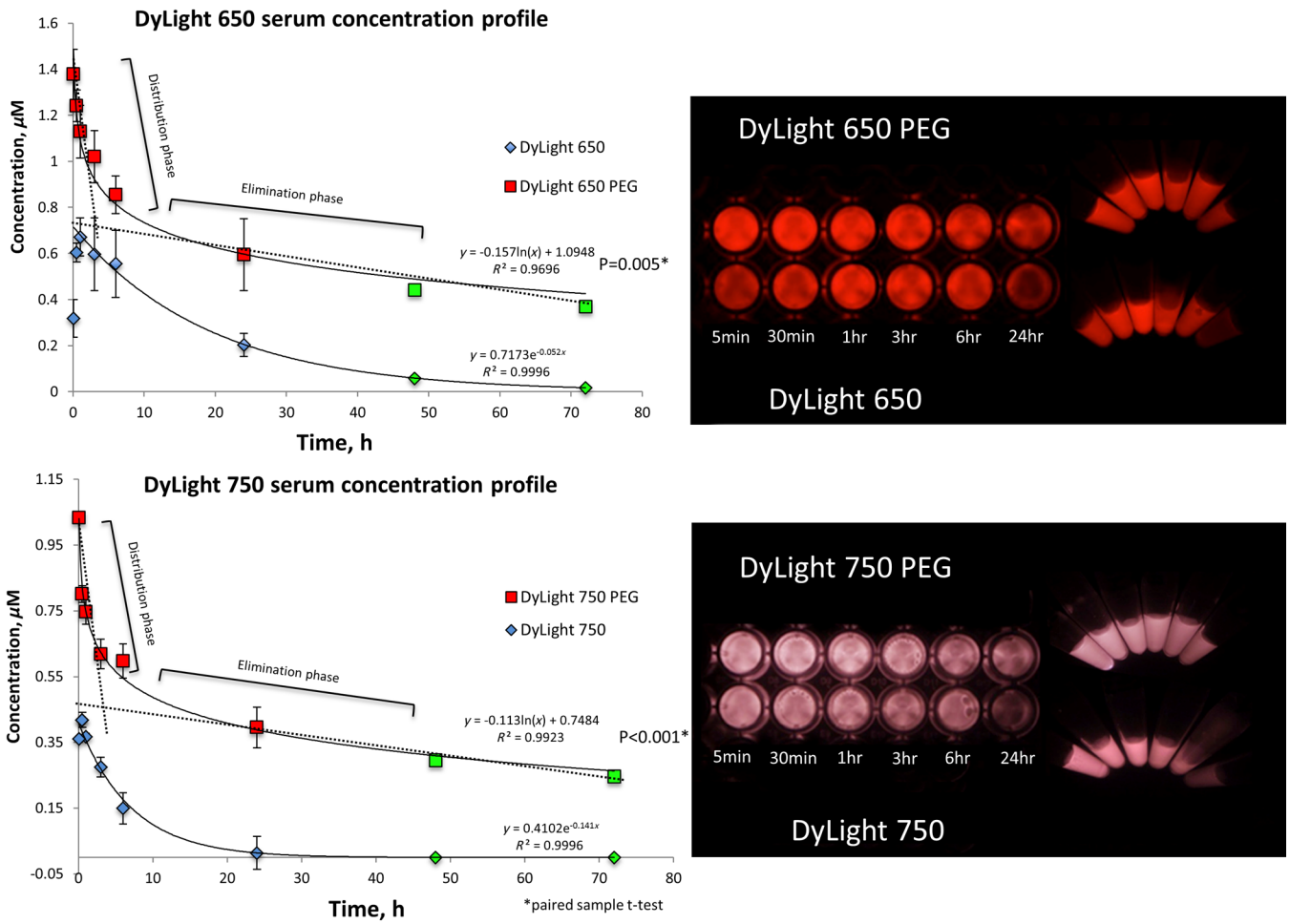

Fig. 2 Elimination profiles of PEGylated and non-PEGylated dye-mAb complexes. PEGylated dyes conjugated to the anti-CEA antibody showed complex third-order elimination curves, whereas non-PEGylated complexes showed first-order elimination. With PEGylated complexes, logarithmic decreases in concentration were observed, whereas with non-PEG complexes more rapid exponential decreases in concentration were observed. Green points were extrapolated, based on the elimination model, out to 72 h with good fit; $R^2 \geq 0.96$ in all scenarios. With the non-PEGylated dyes, an accumulation phase with an increase in concentration to C_{max} was observed, followed by the elimination phase. The PEGylated dyes, however, had high initial serum concentrations followed by a steep decline in concentration, consistent with a redistribution phase followed by an elimination phase. In both dyes, the serum concentrations of the PEGylated complexes were significantly higher than those of the non-PEGylated complexes ($p = 0.005$ for the 650 dyes and $p < 0.001$ for the 750 dyes; $n = 60$ for each). To the right of the graphs, the serum samples collected over a 24-h period are shown, illustrating the difference in elimination patterns.

Table 1 Half-life and volume of distribution of non-PEGylated and PEGylated dyes conjugated to anti-CEA antibodies.

Dye	DyLight 650	DyLight 650 PEG	DyLight 750	DyLight 750 PEG
$t_{1/2}$ (h)	13.3($\pm$1.14)	$\frac{1.63(\pm1.61)}{[C_0]^2}$	4.95($\pm$0.35)	$\frac{7.14(\pm1.04)}{[C_0]^2}$
V_d (L/kg)	0.31	0.07	0.28	0.1

Note: $t_{1/2}$ = half-life. C_0 = dye concentration at time 0; V_d = volume of distribution; L/Kg = liters per kilogram.

2.8 *Tumor Labeling Intensity*

After BxPC-3 tumors had been implanted subcutaneously and allowed to engraft, and grow the mice received either PEGylated or non-PEGylated DyLight 650 or DyLight 750 dyes (2.5 nmol) conjugated to the anti-CEA chimeric antibody, via tail vein injection. The mice were serially imaged using the OV-100 over the course of 2 weeks. The tumor image intensities were analyzed using Image-J software. The average tumor intensities of each dye were recorded and plotted over time. Tumor-to-background contrast (TBC) was obtained by subtracting the average tumor intensity from the average background intensity, as a surrogate for the signal-to-background ratio (SBR). The TBC was recorded and plotted over time.

2.9 *Statistical Analysis*

All statistical analysis was done using SPSS software version 21 (IBM, Armonk, New York). For the pairwise comparisons within the 650 and 750 nm dyes, quantitative variables were calculated using the paired-samples student's t-test and confirmed with the Wilcoxon rank-sum test. A p-value of <0.05 was considered significant. 95% confidence intervals obtained on analysis of the data were configured into all the error bars of the appropriate figures and graphs.

3 Results and Discussion

3.1 *Pharmacokinetics*

PEGylation significantly increased the serum concentrations of the anti-CEA conjugated dyes compared with the non-PEGylated dyes (Fig. 2). Serum concentrations for PEGylated

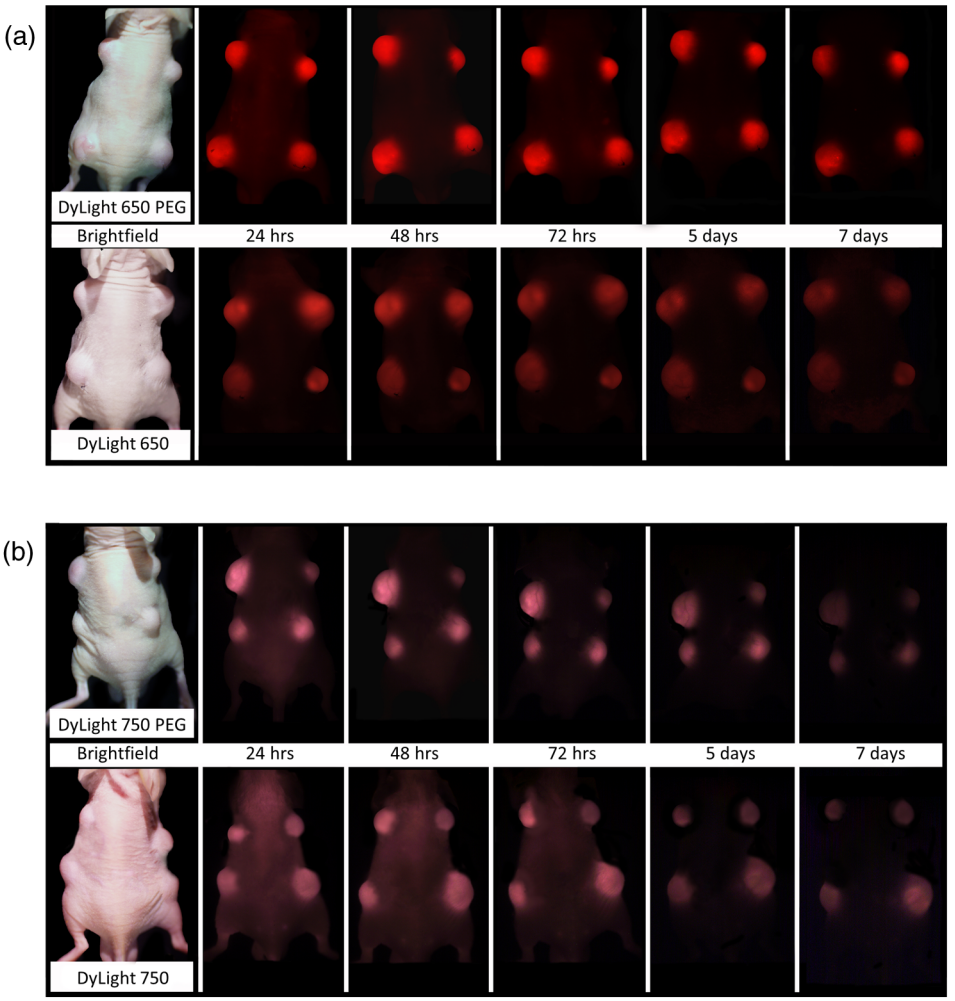

Fig. 3 Tumor intensity of subcutaneously implanted BxPC-3 tumors labeled with the PEGylated and non-PEGylated dyes conjugated to the anti-CEA antibody. In (a), PEGylated and non-PEGylated DyLight 650 was evaluated over the course of 7 days. The PEGylated complexes labeled the tumor significantly brighter and for longer periods ($p < 0.001$; $n = 8$). In (b), PEGylated and non-PEGylated DyLight 750 was evaluated over the course of 7 days. The PEGylated dyes conjugated to anti-CEA labeled the tumor significantly brighter ($p = 0.01$; $n = 8$). Imaging was performed with the OV100.

DyLight 650 were significantly higher than the non-PEGylated form ($p = 0.005$, $n = 60$). Similarly, serum concentration of PEGylated 750 was significantly higher than the non-PEGylated version ($p < 0.001$, $n = 60$).

With the non-PEGylated dyes conjugated to anti-CEA antibodies, there was an accumulation phase before the peak concentration (C_{max}), unlike the PEGylated dyes. The C_{max} for non-PEGylated DyLight 650 and 750 dyes occurred at 1 h and 30 min, respectively, whereas the C_{max} for both PEGylated dyes resulted within 5 min.

Elimination kinetics were also different between the anti-CEA conjugated PEGylated and non-PEGylated dyes. The non-PEGylated dyes followed concentration-independent first-order elimination kinetics, whereas the PEGylated dyes exhibited third-order elimination kinetics (Fig. 2).

3.2 *Rate Equations and Elimination Constant*

With PEGylation of the dyes conjugated to anti-CEA, elimination changed from an exponential decrease in serum concentration over time to a logarithmic decrease in serum concentration over time, calculated using standard rate equations.[9,10]

3.3 *Half-Life*

PEGylated dyes exhibit third-order elimination kinetics that are dependent on initial dye concentration (C_0). Non-PEGylated dyes, however, exhibit first-order elimination kinetics that are independent of initial dye concentration. Both PEGylated dyes conjugated to anti-CEA antibodies had longer half-lives than the non-PEGylated dyes, with DyLight 650 PEG having the longest half-life of the two. PEGylation changed the elimination kinetics and increased the half-lives of the dyes conjugated to anti-CEA from 13.3 h for DyLight 650 to $16.3/(C_0)^2$ h for DyLight 650 PEG and from 4.95 h for DyLight 750 to $7.14/(C_0)^2$ h for Dylight 750 PEG (Table 1).

3.4 *Volume of Distribution*

PEGylation eliminated the accumulation phase of the non-PEGylated dyes. The C_{max} for PEGylated DyLight 650 and 750 dyes conjugated to the anti-CEA antibody were 1 h and 30 min, respectively. The initial serum concentrations (C_0) were higher for the PEGylated dyes versus the non-PEGylated dyes. PEGylation of the DyLight 650 and 750 dyes changed their biodistribution and also decreased their

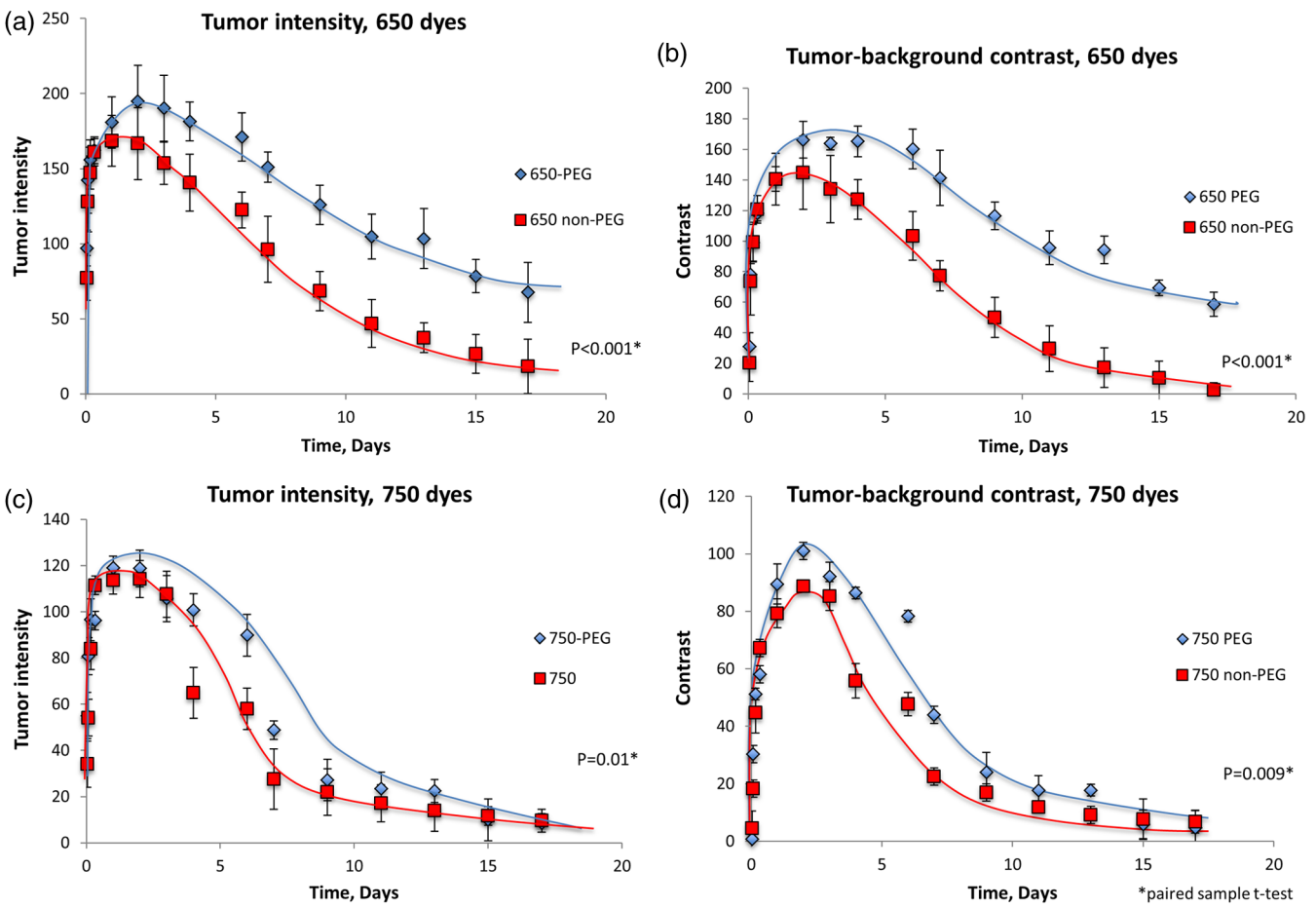

Fig. 4 Graphical representation of tumor and background intensity. In panels (a) and (b), the 650 dyes are evaluated. The PEGylated dye conjugated to the anti-CEA antibody had significantly higher tumor intensity ($p < 0.001$; $n = 8$) and significantly higher contrast between the tumor and background ($p < 0.001$; $n = 8$). In panels (C) and (d), the 750 dyes were evaluated. The PEGylated dye had significantly higher tumor intensity ($p = 0.01$; $n = 8$) and significantly higher contrast between the tumor and background ($p = 0.009$; $n = 8$).

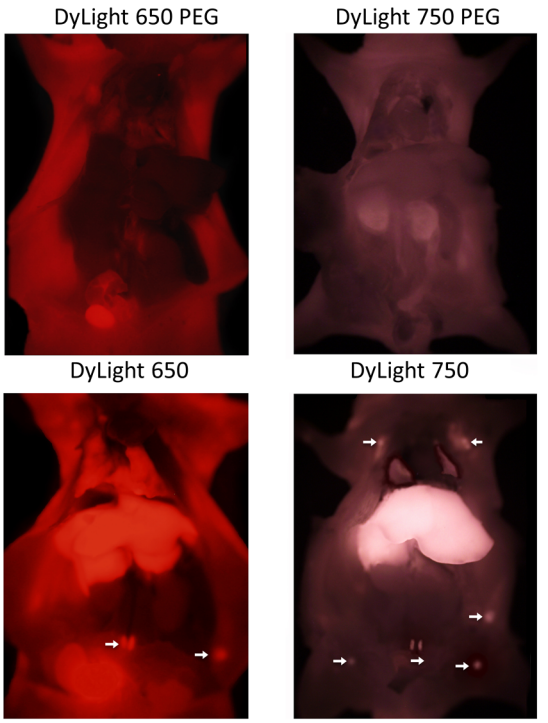

Fig. 5 Biodistribution of PEGylated and non-PEGylated dyes conjugated to anti-CEA antibody. With the PEGylated dyes, there was minimal to no accumulation of dye in the viscera; whereas with the non-PEGylated dyes there was accumulation of dye in the RES organs such as the liver, lung, and lymph nodes. Arrows point to lymph nodes that retained and were labeled by the dye. Imaging was performed with the OV100. The spleen was not clearly imaged with either dye.

volume of distribution from 0.31 to 0.07 for DyLight 650 and DyLight 650 PEG, respectively; and from 0.28 to 0.1 for DyLight 750 and DyLight 750 PEG, respectively (Table 1).

3.5 *Tumor Labeling*

The PEGylated dyes conjugated to the anti-CEA antibody-labeled subcutaneous BxPC-3 tumors significantly brighter than their non-PEGylated counterparts ($P < 0.001$ for the 650 group and $P = 0.01$ for the 750 group) (Figs. 3 and 4). The PEGylated 750 dye conjugated to the anti-CEA antibody labeled the tumor brighter for a longer time than non-PEGylated 750 dye.

3.6 *Tumor–Background Contrast*

The tumor-background contrast was used as a surrogate for the signal to background ratio. For both the 650 and 750 dyes, the TBC was significantly higher for the PEGylated dyes compared with the non-PEGylated dyes ($p < 0.001$ for the 650 dyes and $P = 0.009$ for the 750 dyes) (Fig. 4).

3.7 *Tissue Biodistribution*

PEGylation significantly changed the biodistribution and elimination patterns of both the dyes. PEGylated dyes conjugated to the anti-CEA antibody had significantly lower liver and lung concentrations compared to non-PEGylated dyes (Figs. 5 and 6). Both PEGylated 650 and 750 dyes had significantly lower liver concentrations compared to the non-PEGylated counterparts ($p = 0.03$ for the 650 group and $p = 0.002$ for

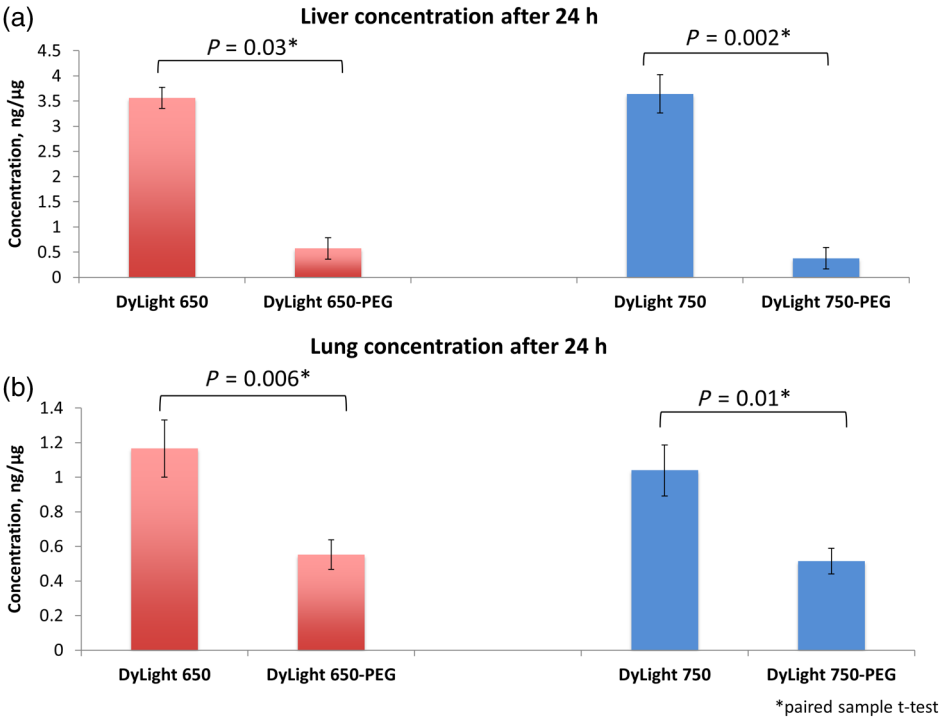

Fig. 6 Tissue concentrations of the dyes 24 h after injection. The liver and lung were assayed to demonstrate tissue accumulation and reticuloendothelial system uptake of the PEGylated and non-PEGylated dyes conjugated to the anti-CEA antibody. The non-PEGylated dyes in both cases accumulated to significantly higher levels than the PEGylated dyes in both the lung ($p = 0.006$; $n = 10$ for the 650 dyes; $p = 0.01$; $n = 10$ for the 750 dyes) and the liver ($p = 0.03$; $n = 10$ for the 650 dyes; $p = 0.002$; $n = 10$ for the 750 dyes).

the 750 group). Similar results were seen in lung tissue ($p = 0.006$ for the 650 group and $p = 0.01$ for the 750 group).

In summary, PEGylation significantly improved the properties of two NIR dyes conjugated to an anti-CEA antibody in a nude mouse model of human pancreatic cancer. The cumulative effects of PEGylation were to increase dye-conjugated anti-CEA antibody half-life, favorably alter the biodistribution, and significantly increase tumor to background contrast. PEGylated dyes conjugated to tumor-specific antibodies should have an important impact in the development of fluorescence guided surgery of cancer,[1,11–26] as these dyes offer the possibility of high fidelity-targeted tumor and metastases labeling.

Acknowledgments

Work supported in part by grants from the National Cancer Institute CA142669 and CA132971 (to M.B. and AntiCancer, Inc).

References

1. A. A. Maawy et al., "Comparison of a chimeric anti-carcinoembryonic antigen antibody conjugated with visible or near-infrared fluorescent dyes for imaging pancreatic cancer in orthotopic nude mouse models," *J. Biomed. Opt.* **18**(12), 126016 (2013).
2. J. Kopecek, "Polymer-drug conjugates: origins, progress to date and future directions," *Adv. Drug Deliv. Rev.* **65**(1), 49–59 (2013).
3. "Final report on the safety assessment of polyethylene glycols (PEGs)-6,-8,-32,-75,-150,-14M,-20M," *Int. J. Toxicol.* **12**(5), 429–457 (1993).
4. C. Özdemir and A. Güner, "Solubility profiles of poly(ethylene glycol)/solvent systems, I: qualitative comparison of solubility parameter approaches," *Eur. Polym. J.* **43**(7), 3068–3093 (2007).
5. S. Dreborg and E. B. Akerblom, "Immunotherapy with monomethoxypolyethylene glycol modified allergens," *Crit. Rev. Ther. Drug Carrier Syst.* **6**(4), 315–365 (1990).
6. A. P. Chapman, "PEGylated antibodies and antibody fragments for improved therapy: a review," *Adv. Drug Deliv. Rev.* **54**(4), 531–545 (2002).
7. T. Yamaoka, Y. Tabata, and Y. Ikada, "Comparison of body distribution of poly(vinyl alcohol) with other water-soluble polymers after intravenous administration," *J. Pharm. Pharmacol.* **47**(6), 479–486 (1995).
8. K. Yamauchi et al., "Development of real-time subcellular dynamic multicolor imaging of cancer-cell trafficking in live mice with a variable-magnification whole-mouse imaging system," *Cancer Res.* **66**(8), 4208–4214 (2006).
9. L. Brunton, J. Lazo, and K. Parker, *Goodman and Gilman's. The Pharmacological Basis of Therapeutics*, McGraw-Hill, New York (2008).
10. K. Connors, *Chemical Kinetics, The Study of Reaction Rates in Solution*, VCH Publishers, New York (1991).
11. M. Bouvet and R. M. Hoffman, "Glowing tumors make for better detection and resection," *Sci. Transl. Med.* **3**(110), 110fs110 (2011).
12. Y. Hiroshima et al., "Successful fluorescence-guided surgery on human colon cancer patient-derived orthotopic xenograft mouse models using a fluorophore-conjugated anti-CEA antibody and a portable imaging system," *J. Laparoendosc. Adv. Surg. Tech. A* **24**(4), 241–247 (2014).
13. Y. Hiroshima et al., "Hand-held high-resolution fluorescence imaging system for fluorescence-guided surgery of patient and cell-line pancreatic tumors growing orthotopically in nude mice," *J. Surg. Res.* **187**(2), 510–517 (2014).
14. S. Kaushal et al., "Fluorophore-conjugated anti-CEA antibody for the intraoperative imaging of pancreatic and colorectal cancer," *J. Gastrointest. Surg.* **12**(11), 1938–1950 (2008).
15. M. McElroy et al., "Imaging of primary and metastatic pancreatic cancer using a fluorophore-conjugated anti-CA19-9 antibody for surgical navigation," *World J. Surg.* **32**(6), 1057–1066 (2008).
16. C. A. Metildi, R. M. Hoffman, and M. Bouvet, "Fluorescence-guided surgery and fluorescence laparoscopy for gastrointestinal cancers in clinically-relevant mouse models," *Gastroenterol. Res. Pract.* **2013**, 290634 (2013).
17. C. A. Metildi et al., "Fluorescence-guided surgery allows for more complete resection of pancreatic cancer, resulting in longer disease-free survival compared with standard surgery in orthotopic mouse models," *J. Am. Coll. Surg.* **215**(1), 126–135; discussion 135–126 (2012).
18. C. A. Metildi et al., "An LED light source and novel fluorophore combinations improve fluorescence laparoscopic detection of metastatic pancreatic cancer in orthotopic mouse models," *J. Am. Coll. Surg.* **214**(6), 997–1007 e1002 (2012).
19. C. A. Metildi et al., "Fluorescently labeled chimeric anti-CEA antibody improves detection and resection of human colon cancer in a patient-derived orthotopic xenograft (PDOX) nude mouse model," *J. Surg. Oncol.* **109**(5), 451–458 (2014).
20. C. A. Metildi et al., "Fluorescence-guided surgery with a fluorophore-conjugated antibody to carcinoembryonic antigen (CEA), that highlights the tumor, improves surgical resection and increases survival in orthotopic mouse models of human pancreatic cancer," *Ann. Surg. Oncol.* **21**(4), 1405–1411 (2014).
21. C. A. Metildi et al., "Fluorescence-guided surgery of human colon cancer increases complete resection resulting in cures in an orthotopic nude mouse model," *J. Surg. Res.* **179**(1), 87–93 (2013).
22. C. A. Metildi et al., "In vivo fluorescence imaging of gastrointestinal stromal tumors using fluorophore-conjugated anti-KIT antibody," *Ann. Surg. Oncol.* **20**(Suppl 3), S693–S700 (2013).
23. H. S. Tran Cao et al., "Tumor-specific fluorescence antibody imaging enables accurate staging laparoscopy in an orthotopic model of pancreatic cancer," *Hepatogastroenterology* **59**(118), 1994–1999 (2012).
24. H. Kishimoto et al., "Tumor-selective, adenoviral-mediated GFP genetic labeling of human cancer in the live mouse reports future recurrence after resection," *Cell Cycle* **10**(16), 2737–2741 (2011).
25. H. Kishimoto et al., "Selective metastatic tumor labeling with green fluorescent protein and killing by systemic administration of telomerase-dependent adenoviruses," *Mol. Cancer Ther.* **8**(11), 3001–3008 (2009).
26. H. Kishimoto et al., "In vivo internal tumor illumination by telomerase-dependent adenoviral GFP for precise surgical navigation," *Proc. Natl. Acad. Sci. U. S. A.* **106**(34), 14514–14517 (2009).

Biographies of the authors are not available.